

Examination of thermally induced deformation of a synchrotron radiation mirror using finite element analysis

C. Lenardi, C. Vecile, R. Vitali, and R. Rosei

Citation: *Rev. Sci. Instrum.* **60**, 1969 (1989); doi: 10.1063/1.1140902

View online: <http://dx.doi.org/10.1063/1.1140902>

View Table of Contents: <http://rsi.aip.org/resource/1/RSINAK/v60/i7>

Published by the [American Institute of Physics](#).

Related Articles

Development of high current Bi and Au beams for the synchrotron operation at the GSI accelerator facility
[Rev. Sci. Instrum.](#) **83**, 02A505 (2012)

Time-resolved soft x-ray absorption setup using multi-bunch operation modes at synchrotrons
[Rev. Sci. Instrum.](#) **82**, 123109 (2011)

Development of a synchrotron biaxial tensile device for in situ characterization of thin films mechanical response
[Rev. Sci. Instrum.](#) **81**, 103903 (2010)

Solid and liquid spectroscopic analysis (SALSA)—a soft x-ray spectroscopy endstation with a novel flow-through liquid cell
[Rev. Sci. Instrum.](#) **80**, 123102 (2009)

Knot undulator to generate linearly polarized photons with low on-axis power density
[Rev. Sci. Instrum.](#) **80**, 085108 (2009)

Additional information on Rev. Sci. Instrum.

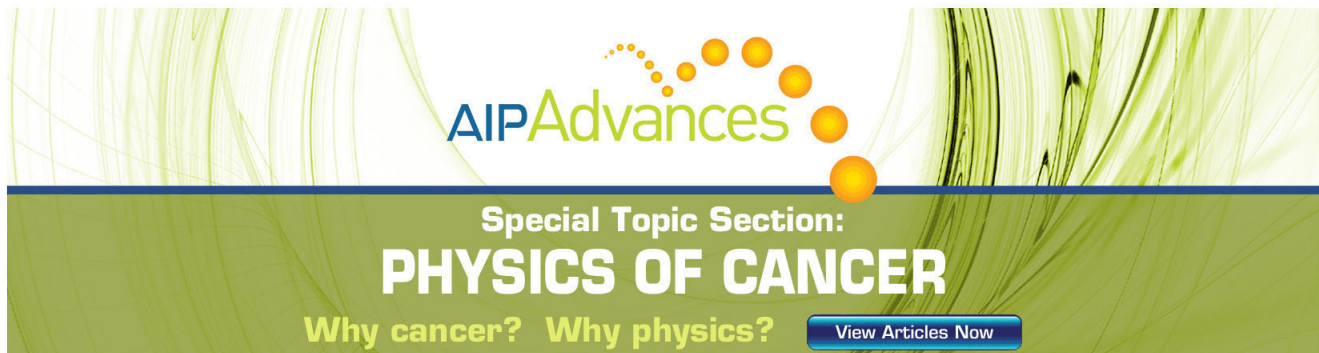
Journal Homepage: <http://rsi.aip.org>

Journal Information: http://rsi.aip.org/about/about_the_journal

Top downloads: http://rsi.aip.org/features/most_downloaded

Information for Authors: <http://rsi.aip.org/authors>

ADVERTISEMENT



AIP Advances

Special Topic Section:
PHYSICS OF CANCER

Why cancer? Why physics? [View Articles Now](#)

Examination of thermally induced deformation of a synchrotron radiation mirror using finite element analysis

C. Lenardi

Area per la Ricerca Scientifica e Tecnologica della Provincia di Trieste, Padriciano 99, Trieste, I-34012 Italy

C. Vecile

Dipartimento di Energetica, Università degli Studi di Trieste, via A. Valerio 10, Trieste, I-34127 Italy

R. Vitali

Control Data Italia S.p.A., Centro Direzionale Milano 2, Segrate, I-20090 Milano, Italy

R. Rosei

Dipartimento di Fisica, Università degli Studi di Trieste, via A. Valerio 2, Trieste, I-34127 Italy and Sincrotrone Trieste S. p. A., Padriciano 99, Trieste, I-34012 Italy

(Presented on 29 August 1988)

A synchrotron radiation mirror is subjected to high thermal loads that cause thermal gradients and surface distortions. The thermally induced deformations can strongly affect the transmission and the energy resolution of insertion device beamlines. We have performed heat transfer calculations and mechanical analyses in order to evaluate surface slope errors of a grazing-incidence mirror. The parameters for these calculations have been chosen according to what will be a typical working situation at the synchrotron radiation facility of Trieste, presently under design. The analysis has been carried out by using the finite element method.

INTRODUCTION

The use of storage ring insertion devices as higher-photon flux sources gives rise to an increase of power density on beamline optical elements. The thermal loads lead to localized thermal gradients and induce internal stresses in the optical components and distortions of the surfaces. These deformations can limit the beamline performance by reducing the photon transmission and the resolving power of monochromators. Calculations,^{1,2} carried out with SHADOW,³ an optical ray-tracing code, in order to simulate the performance of monochromators, show that surface slope errors of about 1 arcsec reduce the limit energy resolution by a factor of ~ 10 and severely affect the transmission of high-energy photons.

In the Elettra design,⁴ a number of VUV and soft x-ray synchrotron radiation beamlines are planned. In these beamlines, a grazing incidence mirror is usually the first optical element and, hence, it receives the highest thermal load. It is important, therefore, to perform precise calculations for estimating the mirror surface figure errors in the presence of the thermal load and give indications for possible variations of beamline performances. They can also help to define a suitable mechanical design.⁵⁻⁸ In Sec. I, we describe how the absorbed power has been calculated according to the Elettra parameters. Section II gives a description of the model of a Ni mirror. A short specification of how the analysis was performed is indicated in Sec. III. Finally, in Sec. IV, results and comments are presented.

I. WORKING CONDITIONS AND THERMAL LOADS

In the case we have considered, the radiation source is an undulator with a period length $\lambda_0 = 5.5$ cm and number

of periods $N = 100$, working at $K = 1$. The electron beam energy is $E = 1.5$ GeV and the current 0.2 A.

The radiation cone, defined by a pinhole, has a half-angle $\vartheta_0 = 0.042$ mrad, corresponding to the central cone angular half-width. The mirror is supposed to be located 10 m away from the radiation source. The beam hits the top surface of the mirror at a grazing angle of 3° and forms on it an elliptical spot (major half-axis $a = 7.6$ mm, minor half-axis $b = 0.4$ mm).

For a correct evaluation of the thermal power which is absorbed by the mirror, we have taken into account the change of reflectivity of the material as a function of the photon energy. In the case of nickel, which we have used in our simulation, the spectral reflectivity for a perfectly smooth mirror is 80% in the 100–500 eV photon energy range; it then goes through two minima corresponding to the L_{III} and L_{II} edges (853 and 870 eV), to reach a value of about 15% and, finally, it decreases to practically zero around 2000 eV.⁹ We have calculated the power density in the central cone for each harmonic from the following formula:

$$\frac{dP}{d\Omega} \left[\frac{W}{\text{mrad}^2} \right] = 7.297 \times 10^{-9} \times \gamma^2 \times N \times I [\text{A}] \times \epsilon_r [\text{eV}] \times F_i(K), \quad (1)$$

where

$$\gamma = \frac{E [\text{GeV}]}{0.511 \times 10^{-3} [\text{GeV}]}, \quad (2)$$

$$\epsilon_r [\text{eV}] = \frac{950 \times E^2 [\text{GeV}]}{\lambda_0 [\text{cm}] \times (1 + K^2/2)} \quad (\text{fundamental energy}), \quad (3)$$

$$F_i(K) = \frac{i^2 K^2}{(1 + K^2/2)^2} \left[J_{(k+1)/2} \left(\frac{iK^2}{4 + 2K^2} \right) - J_{(k-1)/2} \left(\frac{iK^2}{4 + 2K^2} \right) \right]^2 \quad \text{for } i \text{ odd}, \quad (4)$$

$$F_i(K) = 0 \quad \text{for } i \text{ even}. \quad (4')$$

(In the forward direction the frequency spectrum contains only odd harmonics.)

For a certain number of harmonics (first, third, fifth, and seventh), we have evaluated the absorbed fraction of the incident power. For the higher-order of harmonics (above the ninth), we have considered instead that there is total absorption.

The sum of the obtained values gives the total absorbed power; the average value on the irradiated area amounts to 0.03683 W/mm².

II. MODEL DESCRIPTION

The mirror is supposed to be bulk nickel, shaped as a parallelepiped (140 × 60 × 25 mm³) and cooled by water at 20 °C running along the whole bottom surface (film coefficient $h_c = 7.5 \times 10^{-4}$ W/mm² °C). The properties of the material are indicated in Table I.

Under these physical and geometric conditions, a 3D twofold symmetric model can be defined.

The radiation spot size is small compared to the mirror dimensions; therefore, in order to achieve a very high accuracy in the evaluation of the thermal distribution and displacements, a high order of mesh refinement is necessary. This requirement could make the model too cumbersome from a structural point of view, as well as computationally expensive. In order to handle these aspects, the code ABAQUS,¹⁰ which we have used for our analysis, offers a powerful tool: multipoint constraints. This option permits to impose constraints between different degrees of freedom of the model and allows therefore to interface two elements with a single one and then to increase, by repeating the process, the size of the elements (see Fig. 1). For the mesh refinement, we have chosen second order 3D elements.

Using this facility of the program, it has been possible to define a mesh of 380 elements and 2538 nodes (see Fig. 2). It should also be noted that no particular care has been taken to model the irradiated area, apart from the mesh refinement discussed above. In fact, ABAQUS allows to define loading conditions for the most general cases. Any predefined loading condition can be handled via user subroutine option. So, the uniform distributed flux on the elliptical spot has been set by defining the user subroutine DLUX that is able to recognize the mesh points hit by the radiation.

TABLE I. Material properties of nickel

Material	Thermal conductivity	Thermal expansion	Young's modulus	Poisson's ratio	Figure of merit
	k (W/mm °C)	α (1/°C) × 10 ⁻⁶	E (N/mm ²) × 10 ⁶	ν	α/k × 10 ⁻⁶
Ni	0.0889	14.0	1.47	0.31	157.4

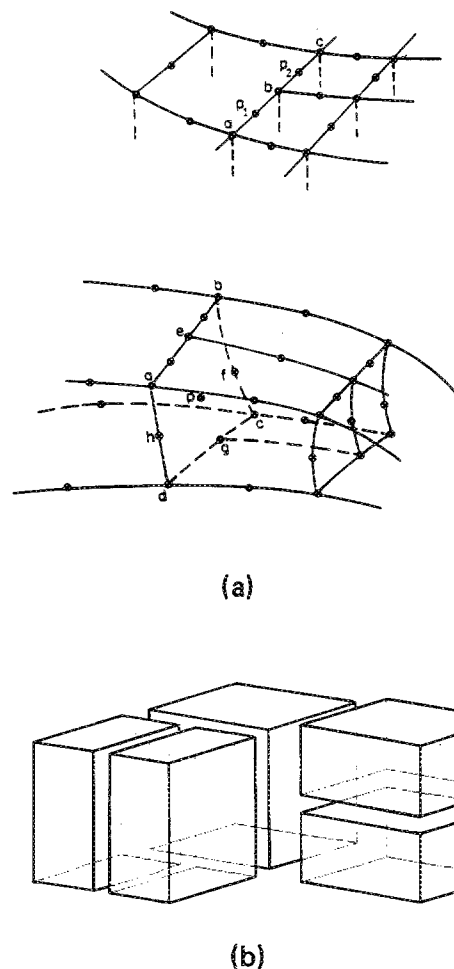


FIG. 1. Multipoint constraints: (a) mesh refinement with second order 3-D elements; (b) an example of the used technique of discretization.

III. HEAT TRANSFER AND MECHANICAL ANALYSIS WITH DIFFERENT BOUNDARY CONDITIONS

A steady-state analysis has been performed in order to evaluate the thermal distribution on the mirror. Thereafter, the temperature field has been taken as input for the stress analysis to obtain the deformed shape of the model.

We have defined three different kinds of boundary conditions, corresponding to various mirror mountings: (1) y and z displacements for two nodes ($x = \pm 70.0$, $y = 0.0$, $z = 10.0$) are constrained; (2) z displacements for the nodes on the bottom surface are constrained; (3) all nodes of the lateral surfaces and the bottom one are fully built in. This

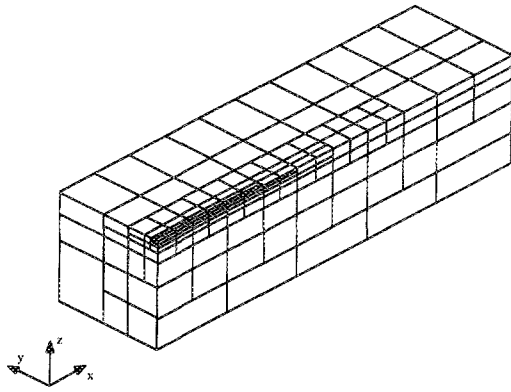


FIG. 2. Partial view of the 3-D mesh model. The mesh is thickened in correspondence to the irradiated area.

last condition is the worst case since it leads to maximum top surface distortion.

IV. RESULTS AND DISCUSSION

Heat transfer analysis gives as maximum value for the temperature 20.52 °C, correctly localized in the center of the radiation spot. The isotherms have an elliptical shape around the irradiated region and tend to become circular far away from the center of the mirror.

In Fig. 3 are indicated the z displacements along the x

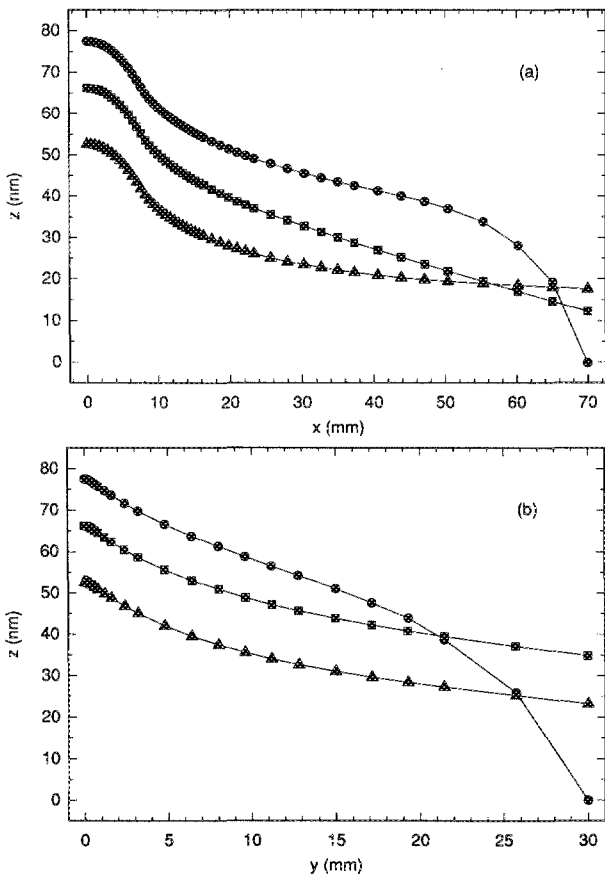


FIG. 3. (a) Displacements along x axis; (b) displacements along y axis. Boundary conditions: ■ two nodes ($x = \pm 70, y = 0, z = 10$) with constrained y and z displacements; ▲ the nodes on the bottom surface with constrained z displacements; ● the nodes on the lateral surfaces and the bottom one are fully built in.

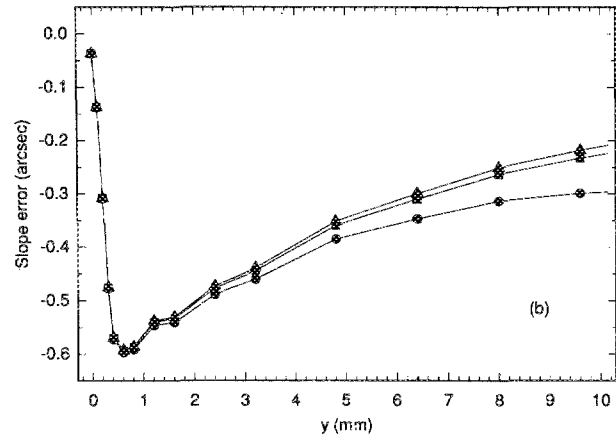
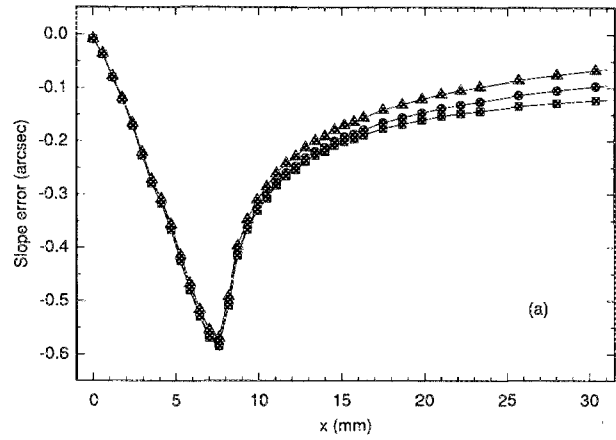


FIG. 4. (a) Slope error along x axis; (b) slope error along y axis. Boundary conditions: ■ two nodes ($x = \pm 70, y = 0, z = 10$) with constrained y and z displacements; ▲ the nodes on the bottom surface with constrained z displacements; ● the nodes on the lateral surfaces and the bottom one are fully built in.

and y axis on the top surface for the three kinds of boundary conditions. As expected, the deformed shape shows that for the third type of boundary conditions, the deformations are larger.

A prominent bump appears exactly where the radiation cone hits the mirror. The slope of this bump is the same for different constraints, as the slope error curves indicate (see Fig. 4). Hence, we can draw a first important conclusion: the various boundary conditions do not modify the figure error shape in the region of interest and, therefore, the working conditions of the mirror remain the same for any different mountings, as well as for constraints that change with time (as long as the mirror dimensions are large with respect to the radiation spot).

The second important result is that the average slope error (in the typical working case we have considered) in the irradiated area amounts to ~ 0.3 arcsec, a value that should not dramatically influence the performance of the beamline. Further work is in progress in order to evaluate the maximum mirror size that affects the bump shape to verify the possibility to reduce the mirror dimensions. Other studies on different cooling systems are planned to estimate their influence on the slope errors.

¹R. Rosei, F. Della Valle, and F. Zanini, Internal Report No. TSRP-IUS-9/86.
²F. Della Valle, F. Zanini, and R. Rosei, Internal Report No. TSRP-IUS-13/86.
³B. Lai and F. Cerrina, Nucl. Instrum. Methods A **246**, 337 (1986).
⁴Draft for the conceptual design for the sincrotrone Trieste, Trieste, February, 1988.
⁵S. Hulbert and S. Sharma, Nucl. Instrum. Methods A **266**, 491 (1988).

⁶M. Dormiani, Nucl. Instrum. Methods A **266**, 507 (1988).
⁷S. Sharma and M. Woodle, Nucl. Instrum. Methods A **266**, 513 (1988).
⁸R. Di Gennaro, W. R. Edwards, and E. Hoyer, SPIE J. **582**, 273 (1985).
⁹B. L. Henke, P. Lee, T. J. Tanaka, R. L. Shimabukuro, and B. K. Fujikawa, At. Data Nucl. Data Tables **27**, 1 (1982).
¹⁰ABAQUS—A general purpose finite element program, Rel. 4.6, Hibbitt, Karlsson, and Sorensen, HKS. Inc., Providence, R.I.